The HELIOS Zodiacal Light Experiment (E 9)

C. LEINERT, H. LINK, E. PITZ, N. SALM, D. KNÜPPELBERG,
Max-Planck-Institut für Astronomie und Landessternwarte Heidelberg

Es wird das Experiment 9 der deutsch-amerikanischen Sonnensonde Helios beschrieben. Es besteht aus 3 Photometern zur Messung des Zodiakallichts bei den ekliptikalen Breiten −15°, −30° und −90° (Südpol der Ekliptik). Die Intensität und Polarisation des Zodiakallichts wird in 3 Farbbereichen gemessen, die in etwa dem internationalen UBV-System entsprechen. Neben der Diskussion der Maßnahmen zur Unterdrückung unerwünschten Streulichts, werden die wesentlichsten optischen und mechanischen Parameter genannt. Es wird Pulszähltechnik verwendet und die Signalverarbeitung beschrieben. Die Stabilität der Sensoren während der ersten 130 Tage der Mission wird diskutiert.

Experiment 9 of the German-American solar probe Helios is described. It consists of 3 photometers to measure the zodiacal light at ecliptical latitudes of −15°, −30° and −90° (south pole of ecliptic). Intensity and polarization of zodiacal light is measured in three wavelength bands corresponding to the international UBV-System. Measures of stray light reduction are discussed and optical and mechanical parameters are given. Pulse counting technique is used and data handling within the experiment is described. The stability of the sensors during the first 130 days of the mission is discussed.

1. SCIENTIFIC OBJECTIVES

The experiment is measuring the zodiacal light, which is sunlight scattered on the extremely thin cloud of interplanetary particles. This cloud extends from near the Sun to the asteroid belt and contains about a dozen micron-sized particles per km^3. From zodiacal light observations it is possible, in principle, to derive the spatial distribution, size distribution and material of the scattering dust particles. The observed intensity is mainly related to the number, the observed colour to the size and the observed polarization to the material of the particles. The Helios experiment is measuring intensity, colour and polarization as a function of Sun – Helios distance for various angles with respect to the sun. The main results to be expected from these measurements are:

(1) spatial distribution of interplanetary dust within 1 A.U.,

(2) detection of changes in the particle mixture of interplanetary dust, if present, and

(3) size and material of interplanetary dust particles.

These informations will allow a better interpretation of existing earthbound observations of zodiacal light.
They also provide a basis for the discussion of the sources of interplanetary dust, which is one of the main questions concerning interplanetary dust.

2. GROSS FEATURES OF THE EXPERIMENT

The experiment consists of three photometers mounted rigidly into the spacecraft with orientations of about 15°, 30° and 90° respectively south of the spacecraft X-Y-plane (see FIG. 1), and of one electronic box. The large baffle systems associated with the photometers are necessary for stray light protection. The total mass of the experiment is 8.93 kg. The maximum power consumption is 9.6 W, including a maximum heater power of 2.2 W for the thermal control of the sensors.

3. OPTICAL SYSTEM

The radiation enters the photometer through an extended stray light baffle, is collected by the objective lens and imaged onto the field stop, which determines the field of view on the sky. Behind the field stop, a field lens images the objective lens onto the aperture stop. The aperture

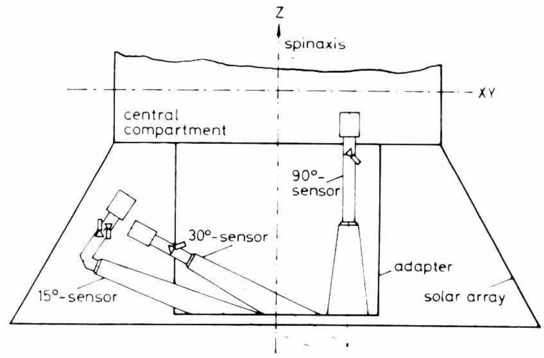

FIG. 1: **Sectional view of the lower spacecraft part with the positions of the zodiacal light photometers**

stop defines the collecting area of the objective lens. Close behind the aperture stop is the photocathode of the photomultiplier. This design not only furnishes a homogeneous illumination of the photomultiplier cathode (by imaging the objective lens onto the cathode), but also images the stray light diffracted or reflected at the mounting of the objective lens outside the aperture stop. Similarly the brightest stray light sources, the rims of the baffle are imaged by the objective lens outside the field stop.
This is essentially a coronograph design and was chosen to give good stray light suppression. Since Helios is exposed to full sunlight and since the sun is 10^{12} to 10^{13} times brighter than the zodiacal light, good suppression of stray light is considered as one main problem of the experiment and as a guideline for the whole design. The suppression of 10^{-14} to 10^{-15} that is needed to have only 1 % stray light contribution to the signal is accomplished in three steps:

First Step:

The photometers are mounted in the shadow zone of the southern spacecraft cone and may only be illuminated by the inner rim of the spacecraft cone, which itself may be exposed to direct sunlight.

Second Step:

Stray light suppression in the baffle system. The light falling into the openings of the baffle systems is caught in the first baffle room (see FIG. 2). The baffle system is designed like

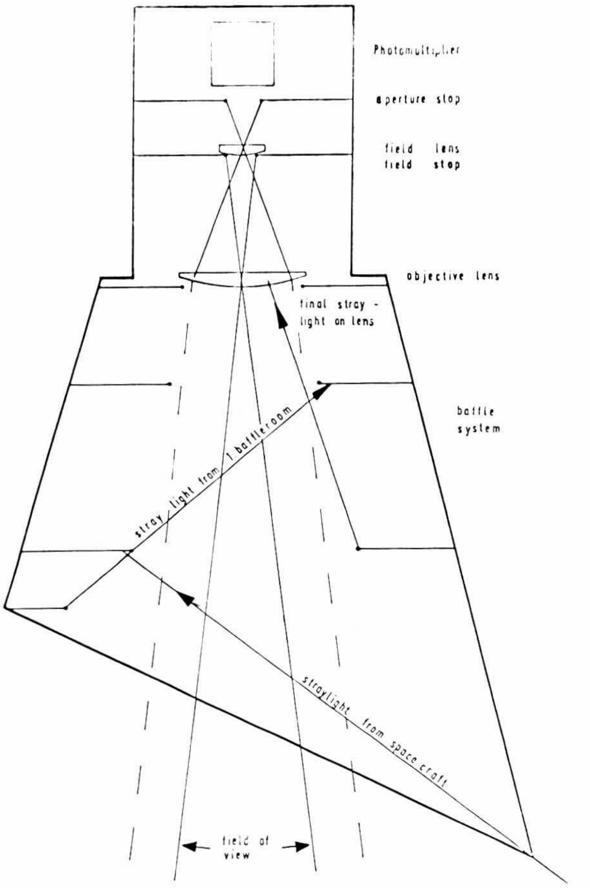

FIG. 2: **Principle of the optical system and stray light suppression**

a trumpet, so that the stray light emerging from the first baffle cannot hit the objective lens directly but only after attenuation by multiple reflections.

Third Step:

The coronograph like design of the optical system prevents stray light falling directly onto the photocathode. To keep the stray light level low, no optical element is allowed between the objective lens and field stop. Since the actual stray light level strongly depends on the amount of dust on the objective lens (it increases by a factor of ten for dusty optics and decreases by a factor of ten for very clean optics), the objective lens was exchanged shortly before

TABLE I: **OPTICAL PARAMETERS OF THE PHOTOMETERS**

	15°-sensor	30°-sensor	90°-sensor
Diameter of aperture (mm)	30	36	36
Focal lenght of obj. lens (mm)	150	200	200
Field of view	1° x 1°	2° x 2°	3° ⌀
Focal lenght of fields lens (mm)	55	55	55
cm^2 x square degree	7.07	40.8	72.1

TABLE II: **DESCRIPTION OF FILTER WHEELS**

Filter wheel	Position	Function (Filter)
15°-photometer color	1	Dark and Calibration
	2	Ultraviolet (UG2)
	3	Blue (BG3 + GG 385)
	4	Visual (GG 10)
15°-photometer polarization	1	Pol.film 0° (quartz)
	2	Pol.film 90° (quartz)
	3	Pol.film 45° (quartz)
	4	Blank (quartz)
30°-photometer	1	Dark and Calibration
	2	Ultraviolet (UG2)
	3	Blue (BG3 + GG 385)
	4	Visual (GG 10)
	5	Blue and pol.film 0° (BG3+GG 385)
	6	Visual and pol.film 0° (GG 10)
	7	Visual and pol.film 90° (GG 10)
	8	Visual and pol.film 45° (GG 10)
90°-photometer	1	Dark and Calibration
	2	Ultraviolet and pol.film 0° (UG2)
	3	Blue + pol.film 0° (BG3 + GG 385)
	4	Visual and pol.film 0° (GG 10)

launch to get rid of the dust which had accumulated during the instrument and system tests. The mechanical design allows this exchange, with fully integrated photometer. The lenses are made from fused quartz (Suprasil) to reduce radiation damage and scintillation. TABLE I gives the basic optical parameters for the three photometers.

The filter wheels are the only movable parts of the experiment. They are driven by permanent magnet stepper motors with 1:16 gear reduction. The gear was introduced to improve positioning and holding torque. The zero position of the filter wheel is recorded by an opto-electronic device in the gear housing. The filter wheels have four positions

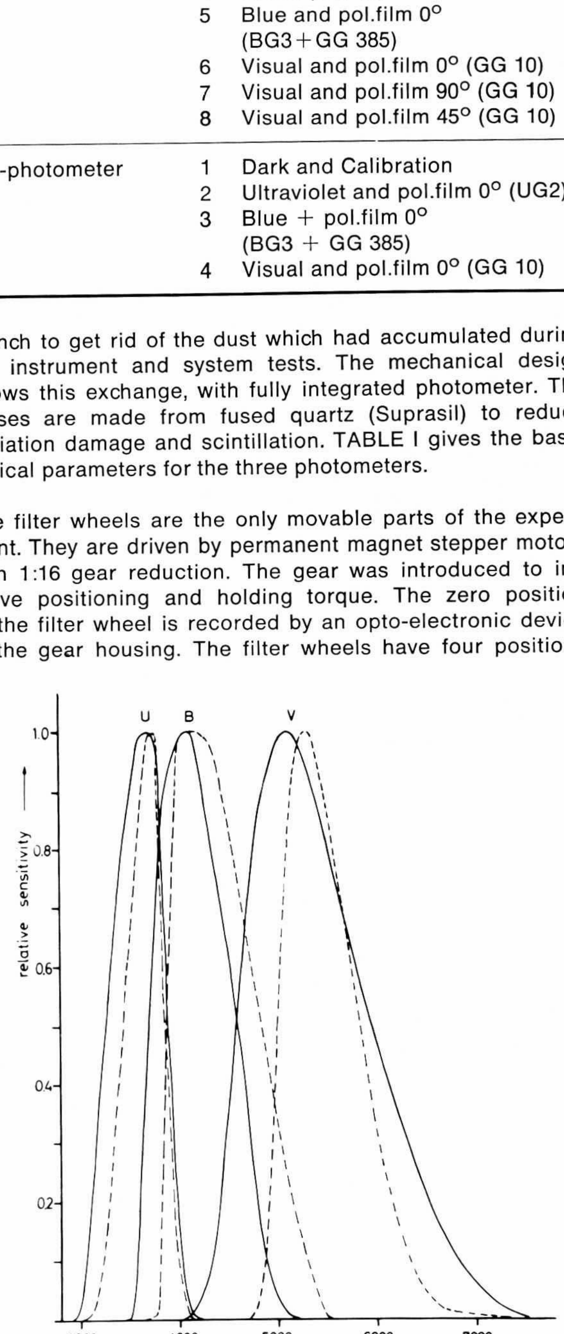

FIG. 3: **Spectral bandpasses compared with the international UBV system**

(8 in the 30°-photometer). In one position the light path is blocked and the light of an internal calibration lamp can be directed onto the photo-multiplier by a small folding mirror mounted on the filter wheel. The other positions contain the filters which define the spectral bandpasses and are Schott glasses with relatively high radiation resistance and low scintillation efficiency. The effective wavelength's for ultraviolet, blue and visual are 3600 Å, 4200 Å and 5300 Å respectively. Broad bandpasses ($\approx \pm$ 500 Å) were selected to allow the use of telescopes with small aperture. For polarization measurements, a polaroid film is used, Polacoat Formula 105 UV, which has a transmission of about 30% in natural light from 3000 Å to 7000 Å. The films are deposited directly on the Schott glasses; in the 15°-photometer they are coated on quartz disks (Suprasil) and mounted in a separate filter wheel, leaving one position blank (quartz). The content of the filter wheels is summarized in TABLE II, and the spectral bandpasses are compared to the international UBV System in FIG. 3. FIG. 4 shows the 15°-photometer together with the central electronic box.

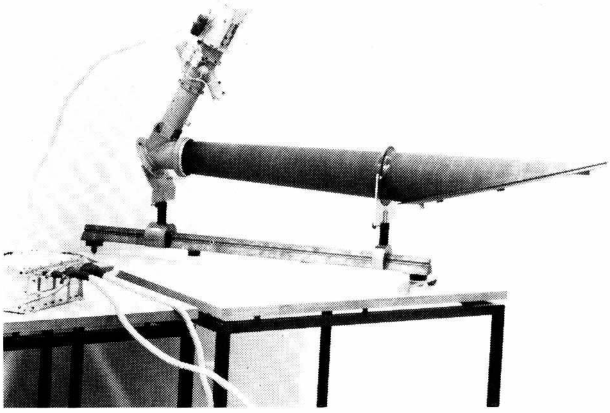

FIG. 4: **15°-photometer (mounted for component tests) together with the central electronic box. On the rear end of the sensor the two filter wheel motors and the analog electronic can be seen**

4. SENSOR UNIT

4.1 Amplifier

The same sensor is used in all three photometers: a head-on photomultiplier, type 541 N of EMR, which has been used in various space experiments. Since the expected dynamical range of the signal is less than 5×10^3, a pulse counting technique is used for ease of data handling. The single electron pulses at the anode of the photomultiplier are amplified and all pulses exceeding a level of 0.5 mV when measured across a resistor of 50 Ω are shaped and fed into a two stage ripple counter, which delivers ervery fourth pulse to the main electronics. The count rate is limited to 11 MHz by a fixed recovery time of the amplifier, introducing a known unlinearity at high photomultiplier pulse rates. For redundancy and to check the proper operation of the amplifier the instantaneous anode current of the photomultiplier is transmitted in an analog housekeeping channel (ratemeter) for each sensor.

4.2 High Voltage Converter

It provides the high voltage supply for the photo-multiplier and the low voltage supply (+ 12 V, −2.5 V) for the amplifier. As the H.-V. converter is located near the sensor only very short cable connections are necessary. The high voltage is individually adjusted ($\approx$ 2500 V) so that the photomultiplier gives a current amplification of 2×10^6. By command, the high voltage can be raised by 300 V to compensate aging of the sensor. The converter is externally synchronized by a 40 KHz pulse train.

5. MAIN ELECTRONIC BOX

In order to measure the angular distribution of the zodiacal light brightness, each revolution of the spacecraft – which means, each scan in the 15° and 30°-photometer – is divided into 32 sectors of different size. The 16 smallest sectors (1/64 revolution) are centered to the sun direction, the 8 largest (1/16 revolution) on the antisolar point and the gap is filled by 8 sectors of the size 1/32 revolution (see FIG. 5). The introduction of large sectors in the regions where a smooth variation of zodiacal light brightness is expected reduces the total number of sectors. Since during the short time of passing one sector the brightness of the zodiacal light cannot be determined with sufficient accuracy, the readings of 513 revolutions are combined for each sector.

In the 90°-photometer, 8 sectors of equal size are introduced to alow polarization measurements. The integration is carried out over 126 revolutions. The technique used to perform these integrations is shown in the block diagram (FIG. 6). Let us assume that the 15°-photometer is measuring and looking into the first sector. Then the output pulses of the 15° photometer sensor unit are going through the input switch into the counter A wich gives a 27 bit semi-logarithmical representation – four bit exponent, 23 bit mantissa – of the accumulated pulse number. As soon as the photometer field of view crosses the boundary to the second sector, the 18 most significant bits of the counter are transferred into the memory A, the nine least significant bits are dropped and the counter is ready to accept the

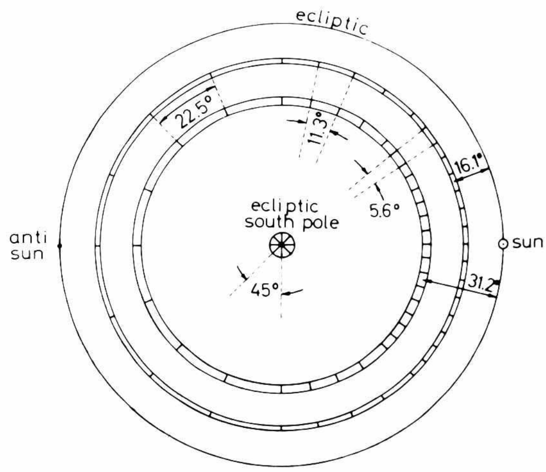

FIG. 5: **Sectoring of the photometer scans on the sky**

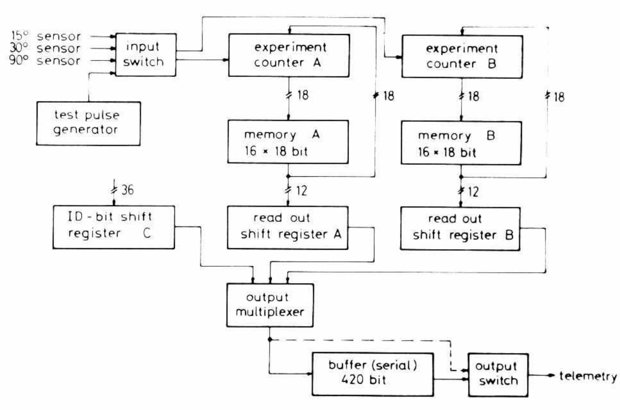

FIG. 6: **Block diagram of the digital electronics**

pulses of sector two. For redundancy, however, the pulses of sector two and all even sectors are handled in the identical counter B and memory B, while all odd sectors go into counter A. The result of any sector is kept in the memory for one revolution of the spacecraft and used as initial value for the counting of pulses during the following revolution, being replaced after that by the new value, etc. until the integration over 513 revolutions is complete. Then the 12 most significant bits for each sector are read out into a buffer and combined with 36 identification bits which describe the status of the experiment. Memory and counter are set to zero, the filter wheel is switched to the next position and a new measurement may begin.

The buffer is read out into the telemetry in a rhythm determined by the momentaneous bit rate and format used for data transmission to the Earth. The data of the 30°-photometer are handled in the same way. For the 90°-photometer, the results of four subsequent measurements are combined in the memory before read-out. Thus the experiment produces science data (as opposed to housekeeping) at a constant rate of $36 + 32 \times 12 = 420$ bit per 516 revolutions. The lacking time from 513 revolutions respectively 4×126 revolutions (integration times) to 516 revolutions is needed to switch the filter wheel(s).

The electronics uses TTL low power circuits. The special counter-memory arrangement has been chosen to give low power consumption, within the limits of this technology. The buffer is made of C-MOS – parts for power reduction. It may be bypassed by command if it fails. In that case the memory is read out directly into the telemetry.

After each cycle of measurements the distribution of the sectors with respect to the counters A and B is reversed. This makes a failure of either part A or B of the electronics less harmful, but has the effect of changing the chronological order of the sectors in the bitstream.

A logic control unit regulates the proper sectoring and sequencing of the measurement. It controls the motor switching, the calibration lamps and the switching of the H-V-converters. It synchronizes the sectoring to the see-sun-direction and regulates the data transfer.

6. CYCLE OF MEASUREMENT

The normal mode of operation consists of continuous repetition of the cycle of measurement. The three photometers are operated in sequence to save power. After switch-on of the 15°-photometer a test measurement is performed during which a pulse train of known frequency is fed into the data handling electronics to check the digital operations. After the dark current and internal calibration measurements the first color filter is moved into the light path for intensity and polarization measurements. The polarization is measured by the method of 3 polaroid settings, with one measurement for each polaroid orientation, the polaroids being exchanged by moving the second filter wheel between the measurements. These measurements are repeated for the second and third colour and followed by a repetition of the dark current and calibration measurements, giving a total of 20 measurements in the 15°-photometer. Each single measurement gives 32 results, one for each of the 32 sectors. In the 30°-photometer 12 measurements are performed beginning and ending with dark current and calibration measurements and using again the method of 3 polaroid settings for the polarization measurements. No test measurement is included because the digital operations are the same as with the 15°-photometer.

Since the 90°-photometer is mounted parallel to the spin axis, the polaroids which stay in fixed position relative to the photometer are rotated by the spin of the spacecraft. Using the method of rotating polaroid, intensity and polarization information for a given color can be obtained in one measurement. Each color is measured three times. Together with test, dark current and calibration measurements, 16 measurements are performed in the 90°-photometer which are combined to 4 read outs.

The time needed for one complete cycle of measurements is $(20 + 12 + 4) \times 516$ revolutions = 5.2 hours. About 40 % of this time are used for test, calibration and dark current measurements.

If the data transmission for this experiment, falls to less than 420 bit/516 revolutions, a new measurement may be completed before the buffer is completely read into the telemetry. In that case, the cycle of measurements is stopped and the next measurement is started only after the buffer has been read out and then refilled with the data of the completed measurement. This mechanism prevents data loss from overwriting in the buffer or the memory but may enlarge the time needed for one cycle of measurements by a factor two or three for very low bit rates.

7. FLIGHT PERFORMANCE

7.1 Stability

As mentioned in section 3, the stability of the sensor sensitivity can be checked by the signal of an internal calibration lamp. FIG. 7 shows for example the signal of the calibration lamp of the 30°-photometer during the first 130 days of the mission. The change of signal is strongly correlated to the variation of the temperature of the sensor which is shown in the lower part of the figure. The two small circles show the expected signal according to ground testing.

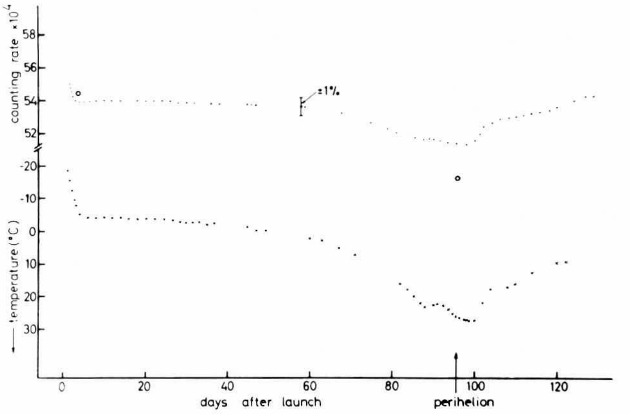

FIG. 7: **Signal of internal calibration lamp and temperature versus time after launch**

7.2 Stray Light

The amount of stray light expected in the data is dependent on the amount of direct sunlight entering the southern spacecraft cone. If the spacecraft is tilted with its spin axis toward the sun line no sunlight can enter the cone and no stray light contribution in the data is expected. However if the spin axis is tilted away from the sun line, the southern rim of the solar array is illuminated by direct sunlight and the antisolar zodiacal light data of the 15°-photometer may be contaminated by stray light. To prove the stray light contribution, two changes of the spacecraft attitude have been performed during the primary mission (one near Earth and one near perihelion) to have both "stray light conditions" during short time spans. The data with and without sunlight in the southern cone show no significant difference which can not be explained by the different star background. We conclude from this, without having reduced the data completely that the stray light contribution in the data is at least smaller than 10 % and the stray light suppression of the photometers works perfectly.

Acknowledgement

This work was supported by Contract RS 21 of the Bundesministerium für Forschung und Technologie (BMFT).